Received: 14 February 2019 | Revised: 9 April 2019 | Accepted: 22 April 2019

DOI: 10.1111/iwj.13137

ORIGINAL ARTICLE

IWJ WILEY

# Release of sodium pyruvate from sacral prophylactic dressings: A computational model

**Ayelet Levy**[1] | **Jan Kottner**[2] | **Amit Gefen**[1]

[1]Department of Biomedical Engineering, Faculty of Engineering, Tel Aviv University, Tel Aviv, Israel

[2]Charité-Universitätsmedizin Berlin, Department of Dermatology and Allergy, Clinical Research Center for Hair and Skin Science, Berlin, Germany

**Correspondence**
Amit Gefen, Department of Biomedical Engineering, Faculty of Engineering, Tel Aviv University, Tel Aviv 69978, Israel.
Email: gefen@tauex.tau.ac.il

**Abstract**

The use of sacral dressings for pressure ulcer prevention is growing rapidly. In addition to their passive biomechanical role in pressure and shear reduction, in the near future, prophylactic dressings may also provide active tissue protection by releasing preventive agents or drugs into skin and deeper tissues. We investigated delivery of sodium pyruvate (NaPy) from an active dressing to potentially protect the sacral skin and underlying tissues in addition. We used four finite element model variants describing different skin roughness levels to determine time profiles of NaPy diffusion from the dressing into the skin layers. The NaPy concentrations for the different modelled cases stabilised after 1 to 6.5 hours from the time of application of the dressings, at 1% to 3% of the NaPy concentration in the dressing reservoir, which is considered potent. We conclude that prophylactic sacral dressings have the potential to deliver NaPy into skin and subdermally, to potentially increase soft tissue tolerance to sustained bodyweight-caused cell and tissue deformations. The time durations to achieve the steady-state potent NaPy dermal concentrations are clinically feasible, for example, for preparation of patients for surgery or for use in intensive care units.

**KEYWORDS**

sodium pyruvate, pressure ulcer prevention, prophylactic dressings, computational simulations

## 1 | INTRODUCTION

The sacrum is the most common anatomical location for developing pressure ulcers (PUs) during supine bed rest.[1] When lying supine, the weight of the pelvis is transferred to the mattress through the pelvic bones, subjecting cutaneous and subcutaneous tissues around the sacrum to sustained elevated deformations, which, if not mitigated or periodically alleviated, may exceed tissue tolerance levels and thereby cause PUs.[2] In the United States and Australia, PUs are also called "pressure injuries," which is the term that is currently recommended by the US National Pressure Ulcer Advisory Panel. Minimising the magnitudes of mechanical loads in soft tissues during weight bearing has long been the main goal in PU prevention (PUP). This is typically addressed by means of pressure-redistributing mattresses, the best of which maximises body immersion and envelopment and hence minimises localised focal body-support contact pressures and stress concentrations subdermally. Over the past few years, the use of dressings as prophylactic measures has grown rapidly and their efficacy in PUP, complementary to adequate mattresses, has been demonstrated via randomised controlled clinical trials, laboratory testing, magnetic resonance imaging, and computational modelling.[2-11] These dressings are designed as smart (passive) mechanical structures that reduce friction with the mattress, absorb shear, and redistribute pressures within weight-bearing soft tissues.[12] However, using prophylactic dressings to provide active

rather than passive tissue protection, that is, as transport vehicles for transdermal delivery of protective and/or treatment agents to the skin and underlying tissues, may have an additional patient benefit.

Local administration of pyruvate compounds and specifically sodium pyruvate (NaPy) appears to be very promising for preventing, arresting, ameliorating, or treating PUs at their earliest stage of cell-level damage.[13-31] Cells regularly produce NaPy, an organic salt of pyruvic acid, as an intermediate metabolite in the glycolysis pathway, and, hence, NaPy is a natural substance within the human body. It is also a standard practice to add NaPy to cell culture media as an energy supplement (ie, as an extra source of carbon in addition to glucose). This laboratory practice has been reported to improve cell survival and to have protective effects on cells against reactive oxygen species in cultures and animal models.[13-16] We hypothesise that the added boost of available energy and anti-oxidative function would allow cells and tissues (predominantly in cutaneous but also in subcutaneous layers) to better tolerate the compromised microvascular conditions and the resulting added oxidative stress in these cases. Furthermore, for similar reasons, NaPy is often being used in facial and body skin care and in cosmetic products as well.[17] The use of NaPy is also common in nutritional products, for example, for fat and weight loss.[18]

In the medical context of tissue protection, there is a plethora of published work regarding the effectiveness of NaPy in protecting brain, lung, kidney, vascular, and eye tissues exposed to traumatic, toxic, ischaemic, or a combination of these insults. Specifically, NaPy has been shown to improve rat renal function after glycerol-induced renal failure,[13] reduce hypoxic-ischaemic and cortical contusion injuries to neonatal and adult rat brains,[19-21] inhibit the progression of cataract,[22] minimise the deficits after myocardial infraction in pigs,[23,24] and enhance lung function in patients with chronic obstructive pulmonary disease.[25] In combination with vitamin E and fatty acids, NaPy reduced cutaneous inflammation and increased healing after viral infection in rodents.[26] Most authors attribute these protective qualities of NaPy to improved cell metabolism, anti-inflammatory and antioxidant effects, and the correction of cellular acidosis.[27-29] In the neurotrauma literature, it has been suggested that supplementation of cells and tissues with NaPy is effective because it reflects the need for additional "fuel" throughout the acute period of increased metabolic demands induced by an injury.[19] Recently, Marom and colleagues[30] demonstrated how small mechanical deformation of fibroblasts and myoblasts grown in monolayers and supplemented with 1 or 5 mM of NaPy prior to and following cellular damage accelerated en masse cell migration and can be applied in wound healing to enhance microscale gap closure. They explained how pyruvate supplementation reduces inflammatory responses, supports mitochondrial oxygen consumption, and, therefore, increases the reserve respiratory capacity, which is correlated with improved motility and increased proliferative potential.[30]

**Key Messages**

- sacral dressings designed for pressure ulcer prevention can be used for delivery of sodium pyruvate (NaPy) to potentially improve skin and subcutaneous tissue tolerance to sustained bodyweight-caused tissue deformations
- subject-specific computational model variants were used to investigate the time profiles of NaPy diffusion from prophylactic dressings into the deep skin layers of two females
- the modelling showed that a steady-state potent NaPy concentration in skin is reached approximately 4 hours after applying the dressings, which is reasonable for usage prior to a scheduled surgery or in intensive care units

All these studies, considered together, point to the potential of NaPy as being a protective agent for cells at the early (microscopic) onset of PUs. Noteworthy is that treating tissues with NaPy several hours after imposing the damaging conditions, such as systemic administration of NaPy 3 hours after inflicting brain ischaemia in rat models, exerts transient benefits but not a persistent protection.[31] Hence, prophylactic pre-treatment of cells and tissues with NaPy is the preferred approach for preventing or reducing cell death and tissue damage in PU development, or, in other words, for improving the tolerance of cells and tissues to PU-inducing conditions. In the context of PUP, it is possible that the added available energy and anti-oxidative capacity provided by NaPy molecules enable cells to maintain their plasma membrane and cytoskeletal integrity under otherwise-damaging sustained mechanical loads. This contribution of the NaPy protectant can be further augmented by a well-designed multilayer preventative dressing structure that would alleviate tissue exposure to the distortions caused by the sustained bodyweight forces.

The aim of this study was to explore how prophylactic sacral dressings, designed for PUP, can also be used for transdermal delivery of NaPy molecules for the purpose of improving skin and subcutaneous tissue tolerance to sustained deformations, as part of an innovative prophylactic technology that will include NaPy release from dressings, as codeveloped by author A.G. (patent pending).[32] For this purpose, we developed four finite element (FE) computational model variants of sacral skin of different roughness levels, and dressings pre-loaded with a known NaPy concentration,

and monitored NaPy diffusion into the skin over a period of 16 hours. Specifically, we have considered the coupled NaPy transport and structural (tissue deformation) behaviours simultaneously, as we believe that such multiphysics modelling and analyses are the way forward in development of future PUP technologies.

## 2 | MATERIALS AND METHODS

In this work, we developed four FE computational model variants of the sacral skin, representing four levels of skin roughness. We have used these model variants to investigate how prophylactic dressings, pre-loaded with NaPy, can be potentially used for transdermal delivery of NaPy molecules. We modelled the application of such novel dressings loaded with a known NaPy concentration, and monitored simulated free NaPy diffusion into the skin for a period of 16 hours.

### 2.1 | Geometry

We used optical coherence tomography (OCT) images of the sacral skin of two female subjects (ages 65 and 66) to generate four two-dimensional anatomical skin models, representing different levels of skin roughness (Figures 1A,B). These subjects were chosen to simulate a scenario of high risk of developing superficial PUs, not necessarily as a result of chronic morbidity but because they may represent adult surgical patients. In the near future and pending additional technological development,[32] surgical patients would be a population that could be effectively protected from PUs by means of NaPy-releasing preventative dressings placed at high-risk anatomical sites during and post-surgery. The subjects signed informed consent forms to the study that were approved by the ethics committee of the Charité-Universitätsmedizin Berlin (approval no. EA1/270/15, 2015). The OCT system Telesto (Thorlabs, Lübeck, Germany) was used to acquire two-dimensional images with a scan length of approximately 5 mm, a lateral resolution of up to 8 μm, and a maximum penetration depth of ~1.5 mm.[33] First, the ScanIP module of the Simpleware software (Synopsys Corporate, Mountain View, California) suite was used[34] to segment the different layers of the skin. Then, assuming that the effective contact area between the skin and NaPy-loaded dressing will strongly affect the resulting NaPy concentrations within the skin, we investigated its effect through the initial roughness level of the stratum corneum (SC): A roughness criterion (R) was set as the maximal vertical distance between the top of the highest fold and the bottom of the lowest valley of the SC, and the four areas of interest were chosen so that $R_1 = 20$ μm, $R_2 = 30$ μm, $R_3 = 40$ μm, and $R_4 = 50$ μm (Figure 1B,C; $R_1$ and $R_2$ are from the same subject, and likewise, $R_3$ and $R_4$ are from the same other individual).[35-37] Then, we assigned

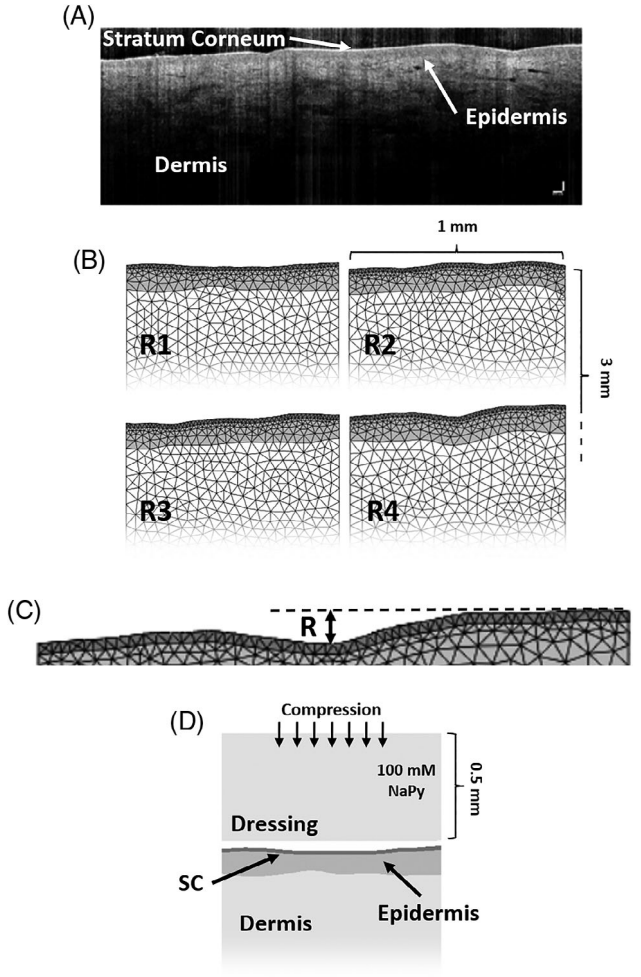


**FIGURE 1** Development of the computational modelling framework used to conduct the studies simulating release of sodium pyruvate (NaPy) from a novel prophylactic dressing: A, optical coherence tomography (OCT) image of the sacral skin of a 67-years-old female used for the OCT-based modelling. B, The four anatomical model variants, representing four levels of skin roughness (R1-R4). C, Zoom-in on the stratum corneum (SC) and epidermis layers of the skin. The roughness criterion was set as the vertical distance between the top of the highest fold to the bottom of the lowest valley. D, The thin-slice transient finite element computational model of NaPy diffusing from the dressing (set as an infinite reservoir here) into the skin

constant minimal thickness to the anatomical model variants so that each of the variants was 1 mm × 3 mm × 0.05 mm and included the SC, epidermis, and dermis layers (Figure 1B). Next, a geometrical representation of a flat dressing was added to each of the model variants, and positioned as close as possible to the rough SC surface (Figure 1D).

### 2.2 | Mechanical and diffusional properties

We considered the dressing and skin layers as biphasic-solute materials in order to be able to simulate the coupled structural response of skin to the (bodyweight) loading and

the diffusion of the NaPy released from the dressing as it compresses onto the skin (under the bodyweight forces). Physical and diffusional properties of the skin layers, dressing, and NaPy molecules were adopted from the literature. Specifically, NaPy molecules were assigned a molecular weight (MW) of 110 g/mol and a neutral chemical charge. Solubility, diffusivity, and free diffusivity of NaPy molecules in the aqueous phase of the dressing and tissues were considered isotropic and set at 100 mg/mL, 0.0005 $mm^2/s$, and 0.001 $mm^2/s$, respectively.[38,39]

The dressing and skin layers were assigned a solid volume fraction of 0.2 and constant isotropic permeability characteristics as follows. Dermal permeability coefficient ($K_p$) of NaPy was calculated using[40]:

$$\log K_p = -2.72 + 0.71 \cdot \left(\log K_{O/W}\right) - 0.0061 \cdot (MW) \quad (1)$$

where $K_{O/W} = -5.05$ and MW = 110.04 g/mol.[39] Because the skin barrier properties are mostly attributed to the SC layer, and given that transepidermal water loss increases 20-fold when the SC is removed, the permeability coefficients of the epidermis and dermis were set as 20 times greater than that of the SC.[41] The final $K_p$ values of skin were set at $2.9322 \cdot 10^{-10}$mm/s for the SC and $5.86445 \cdot 10^{-9}$ mm/s for the epidermis and dermis. $K_p$ of the dressing was set at 0.001 mm/s.

Constitutive laws and mechanical properties of the model components were also adopted from the literature. Specifically, the dressing material was assumed to be isotropic linear-elastic material with an elastic modulus of 19 kPa and a Poisson's ratio of 0.3.[42] The skin layers were assumed to be nearly incompressible (Poisson's ratio of 0.49), non-linear isotropic materials with their large deformation behaviour described using an uncoupled Neo-Hookean material model[43] with a strain energy density function $W$:

$$W = \frac{G_{ins}}{2}\left(\lambda_1^2 + \lambda_2^2 + \lambda_3^2 - 3\right) + \frac{1}{2}K(\ln J)^2 \quad (2)$$

where $G_{ins}$ is the instantaneous shear modulus, $\lambda_i$ ($i$ = 1, 2, and 3) are the principal stretch ratios, $K$ is the bulk modulus, and $J = \det(F)$ where $F$ is the deformation gradient tensor. The instantaneous shear moduli assigned to the skin layers were 839 kPa, 352 kPa, and 7.55 kPa for the SC, epidermis, and dermis, respectively.[44]

## 2.3 | Boundary and material transition conditions

Boundary conditions were chosen to simulate the application of the prophylactic sacral dressing loaded with NaPy in a thin-slice model configuration. The dressing was assigned an initial homogenous concentration of 100 mM and the top surface of the dressing was held at a constant NaPy concentration throughout the simulation, which represented the intra-dressing NaPy reservoir. The front, back, bottom, and side planes of the dressing and skin layers were assigned zero flux across them, and biphasic-solute contact was defined only between the bottom of the dressing and top of the SC, so that NaPy molecules may only leave the dressing into the skin, where contact is established (but not return to the dressing). The front, back, and left planes of the dressing and skin were fixed for perpendicular displacements, while the right surfaces were released to allow adequate convergence of the numerical simulation and relaxation of the osmotic stresses during the diffusional response. The dressing was then lowered by 0.2 mm over two seconds, until contact was established between the dressing and the SC, and NaPy molecules were allowed to translate by diffusion from the dressing into the skin, over a period of 16 hours of simulated application (Figure 2).

## 2.4 | Protocol of simulations

Meshing the model variants was again performed by means of the ScanIP module of Simpleware,[34] using 4-node linear tetrahedral elements (Figures 1B,C). Each model included approximately 1700 elements describing the dressing, 1550

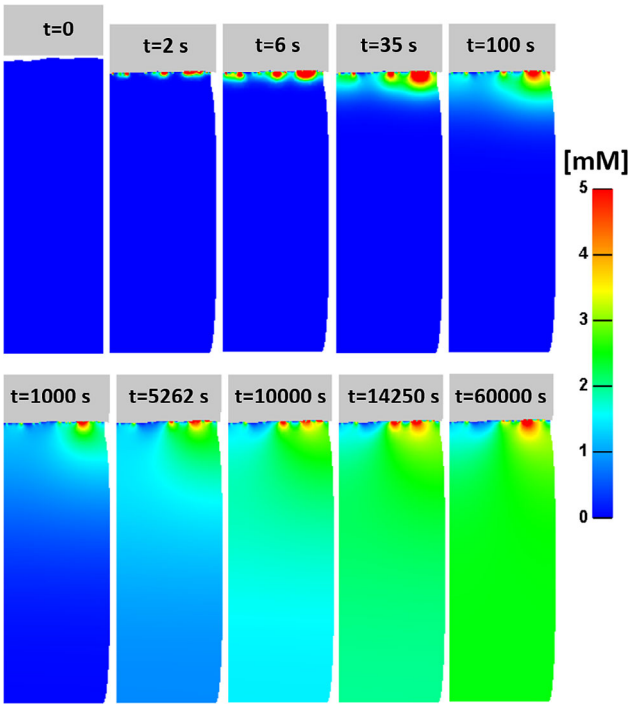


**FIGURE 2** An example time course of the change of concentration of sodium pyruvate (NaPy) molecules entering into the depth of the skin (in model variant R2)

elements describing the SC, 1840 elements describing the epidermis, and 8250 elements describing the dermis.

Simulations were set up in PreView of FEBio (Ver. 1.19), analysed using the Pardiso linear solver of FEBio (http://mrl.sci.utah.edu/software/febio) (Ver. 2.5.0) in its biphasic-solute transient mode, and post-processed using PostView (Ver. 1.10).[43,45] We used a 64-bit Windows 8-based workstation with 2 × Intel Xeon E5-2620 2.00 GHz central processing unit and 64 GB of random access memory for solving the coupled structural-diffusion problems of the NaPy release from a prophylactic dressing. The runtimes for the model variants analysed by means of this computer hardware ranged between 27-36 minutes for all simulations.

## 2.5 | Outcome measures

We compared transient average effective NaPy concentrations in the SC and epidermis layers together, and at depths of 1 mm, 2 mm, and 3 mm into the dermis, for the four examined levels of OCT-measured skin roughness. We further calculated the times until steady-state has been reached, for each model variant and each examined depth of skin. We defined the time required for convergence of a run as the time from the simulated application of the dressing to the first time point where the NaPy concentration level at the examined depth did not change by more than ±10% with respect to the plateau value.

# 3 | RESULTS

An example time course of the NaPy concentration as the substance enters the skin is shown in Figure 2. During the vertical displacement of the dressing, contact area between the dressing and the SC is established and NaPy molecules begin to diffuse from the dressing into the skin. Diffusion persists until the steady state is reached and NaPy concentration stabilises, as expected. The average dermal NaPy flux stabilised after ~5 minutes at 0.35 nmol/cm$^2$ h.

NaPy concentrations in the SC and epidermis layers increased rapidly in all the model variants, and has peaked at 6.92 mM, 4.85 mM, 5.3 mM, and 3.74 mM in model variants R1, R2, R3, and R4, respectively, 7-9 seconds post application of the dressing (Figure 3A). The NaPy concentrations stabilised after 1.15-4.5 hours at 2.98 mM, 2.45 mM, 2.23 mM, and 1.34 mM in model variants R1, R2, R3, and R4, respectively (Figures 3A and 4), that is a coefficient of variation (COV) of 30.4% which reflects the micro-anatomical variability and its impact on the variability of the individualised diffusion responses. Across all the examined dermis depths, NaPy concentrations stabilised after 3-6.6 hours (for all micro-anatomies), at values of 2.88 mM, 2.45 mM, 2.16 mM, and 1.24 mM in model variants R1, R2, R3, and R4, respectively (Figures 3A and 4), which yields a COV of 31.8% (again pointing to the extent of variability in individual diffusion responses). Correspondingly, we found that the relative contact areas between the dressing and the SC reached 54.1%, 51.1%, 44.6%, and 28.7%, in model variants R1, R2, R3, and R4, respectively. The latter demonstrates the potential variability in dressing-skin contact conditions, which is a derivative of the individual skin roughness, being yet another factor that influences the individual diffusion pattern of NaPy into the skin.

Overall, in all but one model variant, NaPy concentrations stabilised faster in the more superficial layers of the skin and slower deeper within the dermis, which could be foreseen given that release is from the NaPy reservoir within

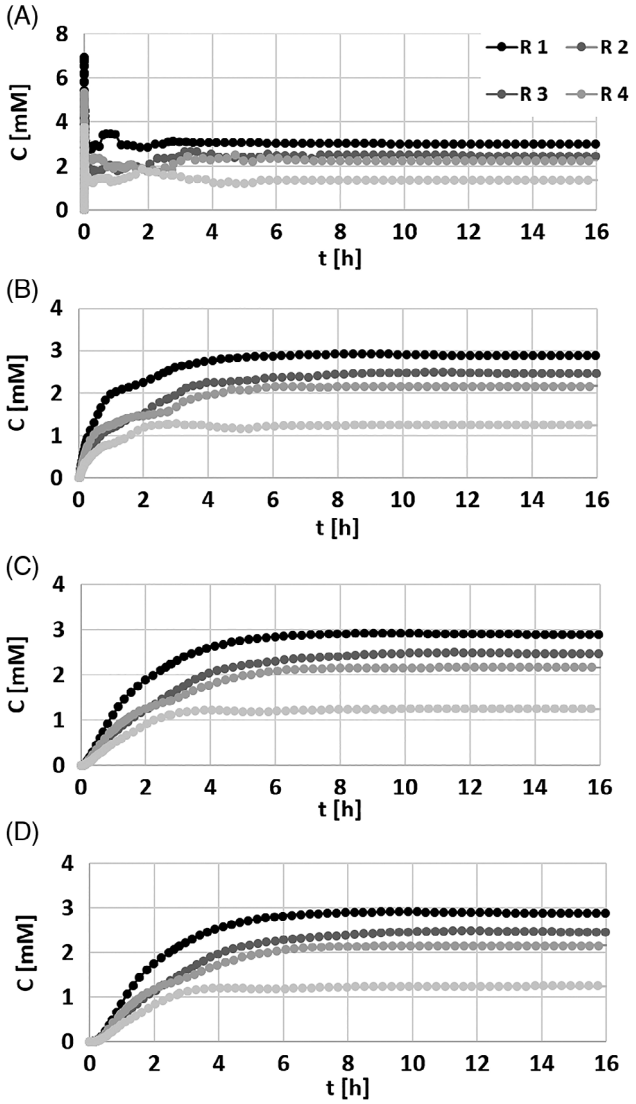


**FIGURE 3** Average sodium pyruvate (NaPy) concentrations recorded during 16 hours of simulated use of the novel NaPy-releasing dressing, in each of the model variants representing four levels of skin roughness (R1-R4), in (A) the stratum corneum and epidermis layers, 1 mm (B), 2 mm (C), and 3 mm (D) deep into the dermis

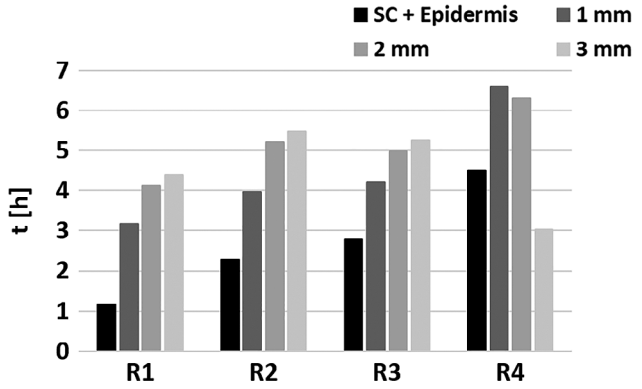


**FIGURE 4** Time from dressing application to sodium pyruvate (NaPy) concentrations reaching a steady state, for the four skin roughness levels (R1-R4), in the stratum corneum and epidermis, and 1, 2, or 3 mm deep into the dermis. Steady state has been defined to occur when the NaPy concentration was within ±10% of the plateau NaPy concentration value

the dressing (Figure 4). For example, in model variant R2, NaPy concentration reached 90% of its final value after 2.28, 3.96, 5.2, and 5.47 hours, in the SC/epidermis, and 1, 2, and 3 mm deep into the dermis, respectively. Additionally, in all but one examined depths, NaPy concentrations stabilised faster in the model variants that represented smoother skin surfaces. For example, at 2 mm into the dermis, the steady state has been reached after 4.13, 5.2, 4.98, and 6.3 hours in model variants R1, R2, R3, and R4, respectively where R1, R2, and R3 are the smoother skins. As mentioned already, this behaviour originates from the quality of attachment of the dressing onto the skin, which typically has less contact area for a more rough skin surface (such as in an aged, wrinkled skin).

## 4 | DISCUSSION

In this study, we developed and used multiple OCT-based FE computational model variants in order to evaluate the transdermal delivery capacities of novel NaPy-loaded prophylactic sacral dressings in different individuals (patent pending by coinventor A.G.).[32] Furthermore, we examined the effects of skin roughness on the resulting diffusional response of the NaPy released from the dressing. We found steady state NaPy concentrations in the dermis, being 1.25%-3% of the concentration loaded in the applied dressing, which is in good agreement with the published data regarding the absorbance capacity of dermal tissues.[46] We further showed that steady state concentrations within the dermis were correlated with the relative contact area between the dressing and the SC, which is a direct outcome of the skin roughness level. This effect was to be expected because the greater the contact area available for diffusion of NaPy, the greater the NaPy flux is across the contact area, and the greater its resulted concentrations in deeper tissue layers. Nevertheless, in real-world conditions, the skin roughness under the dressing will likely decrease as the skin temperature and the SC hydration are expected to increase because of occlusion.[47] Skin hydration and temperature increase are effective and safe penetration enhancers resulting in elevated cutaneous permeation.[48] Our present modelling predictions did not consider these complex skin-dressing interactions at this stage.

In general, the diffusion of molecules through the skin is mostly attributed to the barrier properties of the SC, and also, strongly, on the size of the diffusing molecule, its hydrophilic or hydrophobic nature, and the applied concentration gradient.[48,49] The permeability of intact human skin is significantly decreased for diffusants with a MW above 500 Da.[46] The SC, which is only a few micrometres thick, consists of apoptotic keratinocytes surrounded by keratin-rich lipid bilayers. Because of its hydrophobic nature, the SC barrier will allow the penetration of lipid soluble molecules more readily than water-soluble compounds.[46] Hence, the level of hydration of the SC has a substantial effect on the diffusivity of small hydrophilic molecules, such as NaPy, with greater diffusivity as the hydration level increases.[49] Furthermore, as blood flow in the dermis increases, transport of small hydrophilic molecules increases as well and diffusion to deeper tissues wanes down. The hydration level of the SC as well as the blood flow in the dermis should, therefore, be considered in future modelling of transdermal delivery from prophylactic dressings.

In the medical literature, there are only sparse data regarding the permeability of the SC to NaPy. However, pyruvic acid is commonly used topically on the skin (eg, in the treatment of acne), with obvious potency in deeper skin layers, and hence we assumed that NaPy is able to penetrate the SC spontaneously and in a similar way.[26,50] Furthermore, the results of our simulations agree with those obtained by Wang and Black who examined ex-vivo transdermal delivery of various topical analgesic medications, using Franz Diffusion Cells.[51] They found that the transdermal flux of Diclofenac Sodium that is a similar sodium salt with a MW of 318 g/mol when applied on the skin using a 3% cream reached 0.321-0.943 nmol/cm$^2$ h after 24 hours. They have also measured that a total of 0.846%-1.96% of the applied diclofenac sodium was absorbed in the skin after 48 hours.[51]

NaPy is a relatively small molecule (eg, compared with pyruvate acid) and hence it diffuses freely in the aqueous phase of soft tissues. For example, the corneal penetration of NaPy has been studied in living human eyes 2 hours prior to extraction of the corneal tissue because of cataract surgery. The level of NaPy in control tissue samples of patients who did not receive NaPy eye drops was only 0.145 ± 0.06 mM

(which reflects the natural, baseline corneal NaPy levels, whereas in the group given the NaPy eye drops, it increased to approximately 0.35-0.525 mM.[52] In a later paper by Hegde and colleagues, isotonic or hypotonic NaPy eye drops were applied at a 100 mM concentration and the researchers measured the maximal intraocular NaPy levels, which were 3.1-4.7 mM after 30-60 minutes from the time of administration.[53] These findings are in good agreement with the results of our present simulations with regard to timeframes for plateau of diffusion and concentration levels at the target tissues, however, the use of prophylactic dressings, unlike the application of eye drops or creams, allows for continuous administration of NaPy molecules. Accordingly, release of NaPy from a prophylactic dressing is able to induce a relatively constant concentration in the target soft tissues over time, which is a considerable advantage when the goal is PUP for an estimated specific time frame, such as during (a certain, known type of) surgery. In this context, however, it is important to realise that the NaPy molecules will probably mostly affect the superficial skin and subcutaneous layers, as these ultimately experience the greater, more potent NaPy concentrations (as NaPy is delivered from a dressing which is interfacing the skin). However, because the majority of hospital-acquired PUs are category I & II, the potential protective effect of NaPy administered via such a preventative dressing is likely to be clinically significant, because, as explained above, delivery of the NaPy molecules from the skin surface will most likely affect the epidermal and dermal layers. Additionally, the few hours needed to achieve a steady state potent NaPy concentration in our modelling make a reasonable timeframe for applying such NaPy-loaded sacral prophylactic dressings prior to a planned, scheduled surgery. For example, if the surgery is to be performed in a supine patient, a NaPy-releasing prophylactic sacral dressing might be applied approximately 4 hours prior to anaesthesia (based on the data shown in Figure 3) to potentially increase sacral soft tissues tolerance to the sustained deformations caused by bodyweight forces.

Any type of modelling inevitably involves limitations, which should be discussed. First, we used a single 2D OCT slice to generate the anatomical model of the skin, although the three-dimensional complex structure of the skin surface has a critical effect on the transient penetration profile of molecules through the SC and into the deeper skin layers. Following the 3D to 2D geometrical simplification, the mechanical properties of the layers of the skin were considered isotropic, rather than anisotropic, which again simplifies the spatial mechanical and diffusional response. Furthermore, we used the scans of only two patients, representing four different roughness levels of the outermost SC layer, however, age-related anatomical variations of the thicknesses of the skin layers were not considered and neither did we consider variations in anatomy, mechanical, and diffusional tissue properties.

To conclude, we found that NaPy-loaded dressings can release NaPy molecules, which will likely overcome the SC barrier and may diffuse into deeper layers of the skin. We further found that the time needed to achieve steady-state NaPy concentrations in the dermis was approximately 4 hours, which makes the protective effect of such dressings applicable in preparing a patient for surgery, or for use in intensive care units. We further found that the individual skin roughness might theoretically affect the resulting NaPy concentration in the dermis, although this should be studied further using pre-clinical and clinical trials, considering microclimate and skin barrier alternations that likely occur under the dressing.

## ACKNOWLEDGEMENTS

This work was partially supported by the Israeli Ministry of Science, Technology and Space in the Third Age Program (grant no. 3-12804, awarded jointly to Drs. Daphne Weihs and Amit Gefen in 2016).

## ORCID

*Amit Gefen* https://orcid.org/0000-0002-0223-7218

## REFERENCES

1. Vangilder C, Macfarlane S, Meyer S. Results of nine international pressure ulcer prevalence surveys: 1989 to 2005. *Ostomy Wound Manage*. 2008;54(2):40-54.
2. Levy A, Gefen A. Assessment of the biomechanical effects of prophylactic sacral dressings on tissue loads: a computational modeling analysis. *Ostomy Wound Manage*. 2017;63(10):48-55.
3. Santamaria N, Gerdtz M, Sage S, et al. A randomized controlled trial of the effectiveness of soft silicone foam multi-layered dressings in the prevention of sacral and heel pressure ulcers in trauma and critically ill patients: the border trial. *Int Wound J*. 2015;12(3):302-308.
4. Santamaria N, Gerdtz M, Liu W, et al. Clinical effectiveness of a silicone foam dressing for the prevention of heel pressure ulcers in critically ill patients: border II trial. *J Wound Care*. 2015;24(8):340-345.
5. Forni C, Loro L, Tremosini M, et al. Use of polyurethane foam inside plaster casts to prevent the onset of heel sores in the population at risk. A controlled clinical study. *J Clin Nurs*. 2011;20(5–6):675-680.
6. Ohura T, Takahashi M, Ohura N Jr. Influence of external forces (pressure and shear force) on superficial layer and subcutis of porcine skin and effects of dressing materials: are dressing materials beneficial for reducing pressure and shear force in tissues? *Wound Repair Regen*. 2008;16(1):102-107.
7. Nakagami G, Sanada H, Konya C, Kitagawa A, Tadaka E, Matsuyama Y. Evaluation of a new pressure ulcer preventive

dressing containing ceramide 2 with low frictional outer layer. *J Adv Nurs*. 2007;59(5):520-529.
8. Call E, Pedersen J, Bill B, et al. Enhancing pressure ulcer prevention using wound dressings: what are the modes of action? *Int Wound J*. 2015;12(4):408-413.
9. Kalowes P, Messina V, Li M. Five-layered soft silicone foam dressing to prevent pressure ulcers in the intensive care unit. *Am J Crit Care*. 2016;25(6):108-119.
10. Peko Cohen L, Levy A, Shabshin N, Neeman Z, Gefen A. Sacral soft tissue deformations when using a prophylactic multilayer dressing and positioning system: MRI studies. *J Wound Ostomy Continence Nurs*. 2018;45(5):432-437.
11. Levy A, Schwartz D, Gefen A. The contribution of a directional preference of stiffness to the efficacy of prophylactic sacral dressings in protecting healthy and diabetic tissues from pressure injury: computational modelling studies. *Int Wound J*. 2017;14(6):1370-1377.
12. Gefen A, Kottner J, Santamaria N. Clinical and biomechanical perspectives on pressure injury prevention research: the case of prophylactic dressings. *Clin Biomech (Bristol, Avon)*. 2016;38:29-34.
13. Salahudeen AK, Clark EC, Nath KA. Hydrogen peroxide-induced renal injury. A protective role for pyruvate in vitro and in vivo. *J Clin Invest*. 1991;88(6):1886-1893.
14. Giandomenico AR, Cerniglia GE, Biaglow JE, Stevens CW, Koch CJ. The importance of sodium pyruvate in assessing damage produced by hydrogen peroxide. *Free Radic Biol Med*. 1997;23(3):426-434.
15. Miwa H, Fujii J, Kanno H, Taniguchi N, Aozasa K. Pyruvate secreted by human lymphoid cell lines protects cells from hydrogen peroxide mediated cell death. *Free Radic Res*. 2000;33(1):45-56.
16. Lee JY, Kim YH, Koh JY. Protection by pyruvate against transient forebrain ischemia in rats. *J Neurosci*. 2001;21(20):RC171.
17. Ghersetich I, Brazzini B, Peris K, Cotellessa C, Manunta T, Lotti T. Pyruvic acid peels for the treatment of photoaging. *Dermatol Surg*. 2004;30(1):32-36.
18. Onakpoya I, Hunt K, Wider B, Ernst E. Pyruvate supplementation for weight loss: a systematic review and meta-analysis of randomized clinical trials. *Crit Rev Food Sci Nutr*. 2014;54(1):17-23.
19. Fukushima M, Lee SM, Moro N, Hovda DA, Sutton RL. Metabolic and histologic effects of sodium pyruvate treatment in the rat after cortical contusion injury. *J Neurotrauma*. 2009;26(7):1095-1110.
20. Pan R, Rong Z, She Y, Cao Y, Chang LW, Lee WH. Sodium pyruvate reduces hypoxic-ischemic injury to neonatal rat brain. *Pediatr Res*. 2012;72(5):479-489.
21. Rong Z, Pan R, Chang L, Lee W. Combination treatment with ethyl pyruvate and IGF-I exerts neuroprotective effects against brain injury in a rat model of neonatal hypoxic-ischemic encephalopathy. *Int J Mol Med*. 2015;36(1):195-203.
22. Varma SD, Devamanoharan PS, Rutzen AR, Ali AH, Henein M. Attenuation of galactose-induced cataract by pyruvate. *Free Radic Res*. 1999;30(4):253-263.
23. Kristo G, Yoshimura Y, Niu J, et al. The intermediary metabolite pyruvate attenuates stunning and reduces infarct size in in vivo porcine myocardium. *Am J Physiol Herat Circ Physiol*. 2004;286:517-524.
24. Mallet RT, Sun J, Knott EM, Sharma AB, Olivencia-Yurvati AH. Metabolic cardioprotection by pyruvate: recent progress. *Exp Biol Med*. 2005;230(7):435-443.
25. Votto JJ, Bowen JB, Barton RW, Thrall RS. Inhaled sodium pyruvate improved FEV1 and decreased expired breath levels of nitric oxide in patients with chronic obstructive pulmonary disease. *J Aerosol Med Pulm Drug Deliv*. 2008;21(4):329-334.
26. Sheridan J, Kern E, Martin A, Booth A. Evaluation of antioxidant healing formulations in topical therapy of experimental cutaneous and genital herpes simplex virus infections. *Antiviral Res*. 1997;36(3):157-166.
27. Zhou FQ. Pyruvate in the correction of intracellular acidosis: a metabolic basis as a novel superior buffer. *Am J Nephrol*. 2005;25(1):55-63.
28. Effenberger-Neidnicht K, Brauckmann S, Jägers J, Patyk V, Waack IN, Kirsch M. Protective effects of sodium pyruvate during systemic inflammation limited to the correction of metabolic acidosis. *Inflammation*. 2019;42(2):598-605.
29. Wang Q, van Hoecke M, Tang XN, et al. Pyruvate protects against experimental stroke via an anti-inflammatory mechanism. *Neurobiol Dis*. 2009;36(1):223-231.
30. Marom A, Berkovitch Y, Toume S, Alvarez-Elizondo MB, Weihs D. Non-damaging stretching combined with sodium pyruvate supplement accelerate migration of fibroblasts and myoblasts during gap closure. *Clin Biomech*. 2019;62:96-103.
31. Martín A, Rojas S, Pérez-Asensio F, Planas AM. Transient benefits but lack of protection by sodium pyruvate after 2-hour middle cerebral artery occlusion in the rat. *Brain Res*. 2009;1272:45-51.
32. Weihs D, Gefen A. *Methods and Compositions for Prevention and Treatment of Pressure Ulcers.* International Patent Application, PCT/IL2018/051424; 2018.
33. Trojahn C, Dobos G, Richter C, Blume-Peytavi U, Kottner J. Measuring skin aging using optical coherence tomography in vivo: a validation study. *J Biomed Opt*. 2015;20(4):045003.
34. Simpleware® Ltd. *ScanIP, +FE, +NURBS and +CAD Reference Guide ver. 5.1*; 2012. www.simpleware.com/software. Accessed April 26, 2019.
35. Kottner J, Schario M, Garcia Bartels N, Pantchechnikova E, Hillmann K, Blume-Peytavi U. Comparison of two in vivo measurements for skin surface topography. *Skin Res Technol*. 2013;19(2):84-90.
36. Ohtsuki R, Sakamaki T, Tominaga S. Analysis of skin surface roughness by visual assessment and surface measurement. *Opt Rev*. 2013;20(2):94-101.
37. Askaruly S, Ahn Y, Kim H, et al. Quantitative evaluation of skin surface roughness using optical coherence tomography in vivo. *IEEE J Quantum Elect*. 2019;25(1):1-8.
38. Søgaard LV, Schilling F, Janich MA, Menzel MI, Ardenkjaer-Larsen JH. In vivo measurement of apparent diffusion coefficients of hyperpolarized $^{13}$C-labeled metabolites. *NMR Biomed*. 2014;27(5):561-569.
39. National Center for Biotechnology Information. PubChem Compound Database; CID=23662274. https://pubchem.ncbi.nlm.nih.gov/compound/23662274 Accessed November 11, 2018.
40. Bartzatt R. Determination of dermal permeability coefficient (Kp) by utilizing multiple descriptors in artificial neural network analysis and multiple regression analysis. *J Sci Res Rep*. 2014;3:2884-2899.

41. Machado M, Salgado TM, Hadgraft J, Lane ME. The relationship between transepidermal water loss and skin permeability. *Int J Pharm*. 2010;384(1–2):73-77.
42. Levy A, Frank MB, Gefen A. The biomechanical efficacy of dressings in preventing heel ulcers. *J Tissue Viability*. 2015;24(1):1-11.
43. FEBio: finite element for biomechanics, theory manual ver. 1.5; 2012. http://mrl.sci.utah.edu/software/febio. Accessed April 26, 2019.
44. Geerligs M. in vitro Mechanical Characterization of Human Skin Layers: Stratum Corneum, Epidermis and Hypodermis [doctoral dissertation]. Eindhoven, the Netherlands: Eindhoven University of Technology; 2009.
45. Maas SA, Ellis BJ, Ateshian GA, Weiss JA. FEBio: finite elements for biomechanics. *J Biomech Eng*. 2012;134(1):5-11.
46. JD1 B, Meinardi MM. The 500 Dalton rule for the skin penetration of chemical compounds and drugs. *Exp Dermatol*. 2000;9(3):165-169.
47. Kottner J, Black J, Call E, Gefen A, Santamaria N. Microclimate: a critical review in the context of pressure ulcer prevention. *Clin Biomech*. 2018;59:62-70.
48. Trommer H1, Neubert RH. Overcoming the stratum corneum: the modulation of skin penetration. A review. *Skin Pharmacol Physiol*. 2006;19(2):106-121.
49. Chen L, Lian G, Han L. Use of "Bricks and Mortar" model to predict transdermal permeation: model development and initial validation. *Ind Eng Chem Res*. 2008;47:6465-6472.
50. Cotellessa C, Manunta T, Ghersetich I, Brazzini B, Peris K. The use of pyruvic acid in the treatment of acne. *J Eur Acad Dermatol Venereol*. 2004;18(3):275-278.
51. Wang X, Black L. Ex vivo percutaneous absorption of ketamine, bupivacaine, diclofenac, gabapentin, orphenadrine, and pentoxifylline: comparison of versatile cream vs. reference cream. *Int J Pharm Compd*. 2013;17(6):520-525.
52. Chandra P, Hegde KR, Varma SD. Possibility of topical antioxidant treatment of cataracts: corneal penetration of pyruvate in humans. *Ophthalmologica*. 2009;223(2):136-138.
53. Hegde KR, Kovtun S, Varma SD. Intraocular penetration of pyruvate following its topical administration in mice. *Mol Cell Biochem*. 2010;38(1–2):87-90.

**How to cite this article:** Levy A, Kottner J, Gefen A. Release of sodium pyruvate from sacral prophylactic dressings: A computational model. *Int Wound J*. 2019;16:1000–1008. https://doi.org/10.1111/iwj.13137